ANL-5766
Reactors - General
(TID-4500, 14th Ed.)
AEC Research and
Development Report

ARGONNE NATIONAL LABORATORY
P. O. Box 299
Lemont, Illinois

A GAMMA-RAY ATTENUATION METHOD FOR VOID FRACTION DETERMINATIONS IN EXPERIMENTAL BOILING HEAT TRANSFER TEST FACILITIES

by

H. H. Hooker and G. F. Popper

Reactor Engineering Division

November, 1958

Operated by The University of Chicago
under
Contract W-31-109-eng-38

DISCLAIMER

TABLE OF CONTENTS

A GAMMA-RAY ATTENUATION METHOD FOR VOID FRACTION DETERMINATIONS IN EXPERIMENTAL BOILING HEAT TRANSFER TEST FACILITIES

H. H. Hooker and G. F. Popper

ABSTRACT

Gamma rays emanating from a radioactive source are beamed through and are attenuated by steam-water mixtures contained in a simulated reactor flow channel. The emergent radiation is detected by a scintillation crystal-photomultiplier tube assembly.

An expression is developed which yields the void fraction when the detector output with the channel empty, filled with water, and containing the mixture in question, is known.

The principal sources of errors inherent in the method are analyzed and their magnitudes computed for a specific test facility. With a uniform bubble distribution in this facility, the maximum possible error in void fraction is approximately ± 0.03.

The method is also applied to three idealized preferential phase distributions simulated in Lucite. However, the large discrepancy between calculated and measured void fractions illustrates the need for more refined experimental techniques where non-uniform distribution of voids are encountered. Such techniques are being developed.

I. THEORY

The accurate determination of the volumetric steam void fraction, α, of water-steam mixtures is essential to the design of water-moderated boiling reactors. The technique of measurement to be described is based upon the principle that, as gamma rays pass through matter, the photons are absorbed and the intensity decreases exponentially with the distance traversed. The extent of absorption is proportional to the intensity of the radiation and to the thickness of the medium at a given point:

$$dI = -\mu I \, ds \quad , \tag{1}$$

where

I = intensity of radiation (r/hr)
μ = linear absorption coefficient of the material traversed (cm^{-1})
ds = thickness of material traversed (cm).

When a collimated beam of monoenergetic gamma rays of initial intensity I_0 passes through a material s centimeters thick, the intensity of the emergent beam is obtained by integrating Eq. (1):

$$I = (I_0) \exp(-\mu s) \quad . \tag{2}$$

II. APPLICATION TO STEAM-WATER MIXTURES

In the determination of α, it is assumed that (1) the gamma radiation is monoenergetic; (2) the steam-water mixture can be represented by layers of steam and water perpendicular to the incident radiation: and (3) only the radiation passing through the steam-water mixture reaches the scintillation crystal. In present practice radiation from a source passes through a vessel or flow channel containing water and steam bubbles. The attenuated radiation then impinges on a scintillation crystal which is mounted on the face of a photomultiplier tube. The crystal-tube assembly is enclosed to prevent the entrance of extraneous light. The current output of the photomultiplier tube is amplified and recorded on an Esterline-Angus recorder. This is known as the integrated intensity method of measuring radiation.

With reference to the illustration, and assuming that a collimated beam of monoenergetic radiation passes through structural materials, water, and steam in any order, the intensity of the exit radiation is given by:

$$I = (I_0) [\exp(-\mu_1 d)] [\exp(-\mu_2 x)] [\exp -\mu_3 (x_0 - x)]$$
$$= (I_0) [\exp -(\mu_1 d + \mu_3 x_0)] [\exp \{-x(\mu_2 - \mu_3)\}] \quad . \tag{3}$$

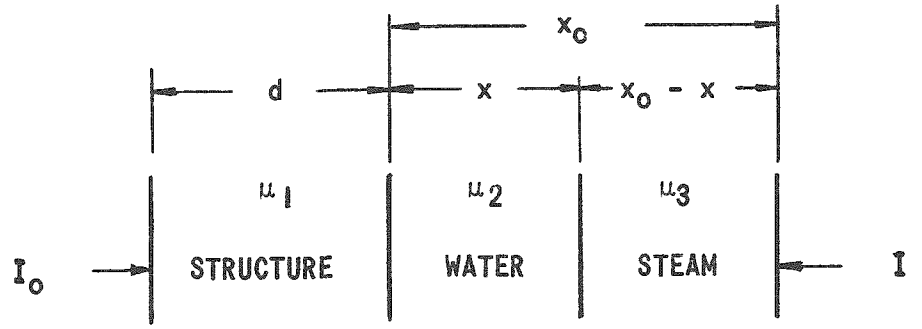

Under conditions of constant temperature and pressure, μ_1, μ_2, μ_3, d, and x_0 are constant; then

$$I = (k_1)\ (I_0)\ \exp\ (-\mu' x) \quad , \tag{4}$$

where

k_1 = a constant = $\exp\ \{-(\mu_1\ d + \mu_3\ x_0)\}$

$\mu' = \mu_2 - \mu_3$.

If A is the perpendicular area of the channel "seen" by the detector, the amount of radiation passing through A is given by

$$\Phi = IA$$

$$= (k_1)\ (A)\ (I_0)\ \exp\ (-\mu' x) \quad . \tag{5}$$

If the resulting radiation, Φ, is allowed to impinge on a fluorescent crystal whose light output is proportional to the amount of exciting radiation,

$$\Phi_V = f_1(T)\ \Phi$$

$$= (k_1)\ f_1(T)\ (A)\ (I_0)\ \exp\ (-\mu' x) \quad , \tag{6}$$

where

Φ_V = amount of visible light

$f_1(T) = \dfrac{\Phi_V}{\Phi}$ = conversion efficiency of the scintillation crystal.

The conversion efficiency can be assumed to be constant over the range of fluxes involved, but its value is a function of temperature.[1,2,3]

If a fixed fraction, k_3, of the generated light falls on the photocathode of a photomultiplier tube, the tube anode current output i is:

$$i = (k_3)\ [f_2(T)]\ (v_h)^7\ (\Phi_V)$$

$$= (k_1)\ [f_1(T)]\ (k_3)\ [f_2(T)]\ (v_h)^7\ (A)\ (I_0)\ \exp\ (-\mu' x) \tag{7}$$

where

$f_2(T)$ = a value determined by the conversion efficiency of the photomultiplier tube and the units in which voltage is expressed, and is also temperature dependent

v_h = photomultiplier tube supply voltage.

It is apparent from the term $(v_h)^7$ that the tube supply voltage must be regulated with seven times the precision required in the output of the photomultiplier tube.

The current signal, (Eq. 7), is fed into a linear amplifier whose output voltage v is:

$$v = (k_5)\ (i) \tag{8}$$

$$= (k_5)\ (k_1)\ [f_1(T)]\ (k_3)\ [f_2(T)]\ (v_h)^7\ (A)\ (I_0)\ \exp\ (-\mu' x)$$

$$= [f_3(T)]\ \exp\ (-\mu' x)$$

where

k_5 = transfer characteristic of the current amplifier

$f_3(T) = (k_1)\ [f_1(T)]\ (k_3)\ [f_2(T)]\ (k_5)\ (v_h)^7\ (A)\ (I_0)$.

By definition

$$\alpha = \frac{x_0 - x}{x_0} \tag{9}$$

or

$$x = (x_0)\ (1 - \alpha) \quad .$$

Substitution of Eq. (9) into Eq. (8) gives

$$v = [f_3(T)]\ \exp\ -\ \{\mu' x_0\ (1 - \alpha)\} \tag{10}$$

$$= [f_3(T)]\ [\exp\ (-\mu' x_0)]\ [\exp\ (\mu'\ \alpha\ x_0)] \quad .$$

When

$$\alpha = 1,$$

then

$$v = v_e$$

or, from Eq. (10),

$$v_e = f_3(T) \quad , \tag{11}$$

where

v_e = actual output voltage for an empty channel.

When

$$\alpha = 0,$$

then

$$v = v_f$$

or, from Eq. (10),

$$v_f = [f_3(T)] \exp(-\mu' x_0) \quad , \tag{12}$$

where

v_f = actual output voltage for a full channel.

Substitution of Eqs. (11) and (12) into Eq. (10), gives

$$v = v_f \left(\frac{v_e}{v_f}\right)^{\alpha} \quad . \tag{13}$$

Taking the logarithm of both sides of Eq. (13), there is obtained

$$\ell n\, v = \ell n\, v_f + \alpha\, \ell n \left(\frac{v_e}{v_f}\right) \tag{14}$$

or

$$\alpha = \frac{\ell n\, (v/v_f)}{\ell n\, (v_e/v_f)} \quad . \tag{15}$$

Thus a plot of α as a function of $\ell n\, v$ should produce a straight line. If the values of v_e and v_f are known, intermediate values of α may be obtained from such a linear plot on semi-log paper. This involves reading the instrument deflection from the chart, plotting the empty and full deflections as logarithmic coordinates, connecting these points with a straight line, and reading α for any deflection from this plot.

III. DESCRIPTION OF APPARATUS

Figure 1 is a plan view of the apparatus used to determine the void fraction in two-phase mixtures contained in an electrically heated, vertical, rectangular, stainless steel flow channel. The source and detector components are mounted on a carriage (Fig. 2) which traverses the length of the

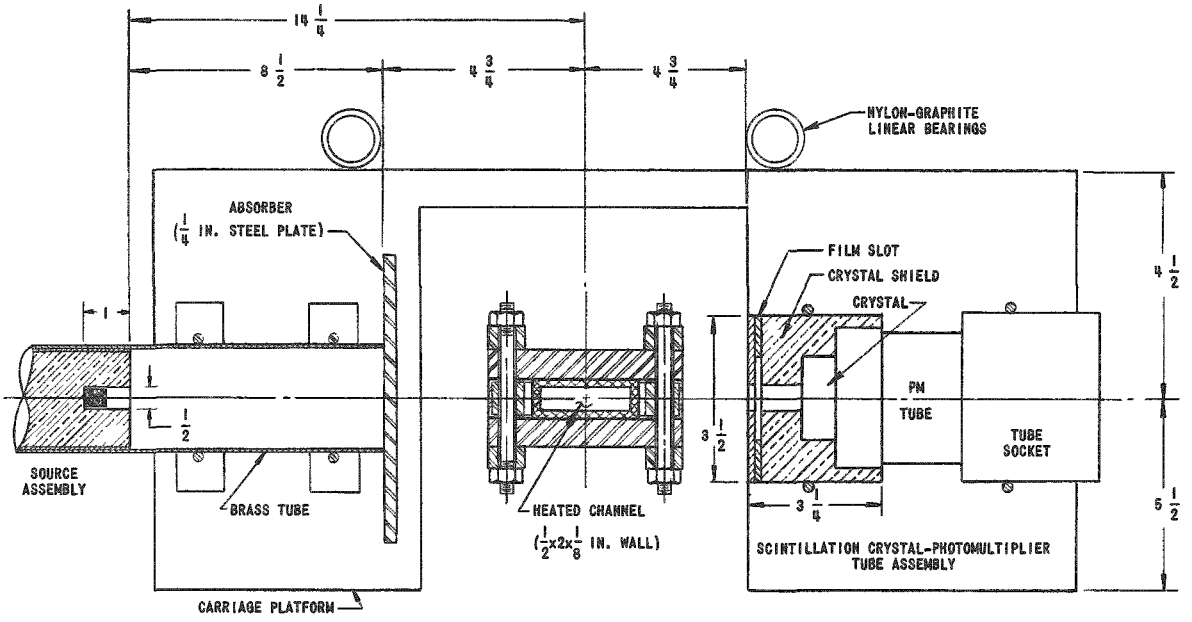

NOTE: ALL DIMENSIONS IN INCHES

FIG. 1
PLAN VIEW OF DENSITY CARRIAGE ASSEMBLY

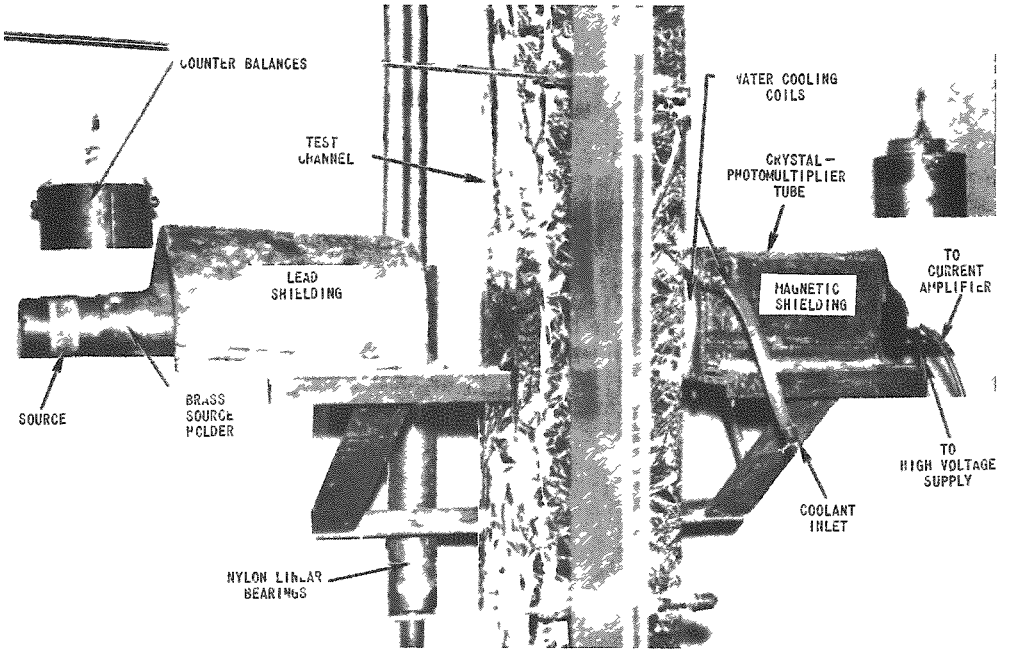

Fig 2
DENSITY CARRIAGE ASSEMBLY

channel. The carriage is rigidly affixed to four nylon-graphite linear bearings which ride on two rods (1 in. dia.). The rods are fastened to the heated channel to minimize misalignment between the carriage and channel due to thermal expansion. A drive motor and linkage, and counterbalancing weights, are provided for positioning the carriage at any desired location along the length of the channel.

A. Gamma-Ray Source

The source consists of a thulium pellet (0.190 in. dia.) enclosed in an aluminum container and irradiated to produce 9 r/hr at a distance of 6 in. in air. The end product is the isotope thulium-170 which has a half-life of approximately 129 days and two energy peaks: 0.053 Mev and 0.084 Mev. To provide the monoenergetic radiation necessary for these measurements, the lower energy K-X-ray peak must be adequately absorbed. This is accomplished by placing an absorber equivalent to at least 1 gm/cm^2 of lead between the source and the steam-water mixture being measured.(4) In the present apparatus a 0.25-in. thick steel plate is used for this purpose. A cut-away drawing of the source, shield, and collimator is shown in Fig. 3.

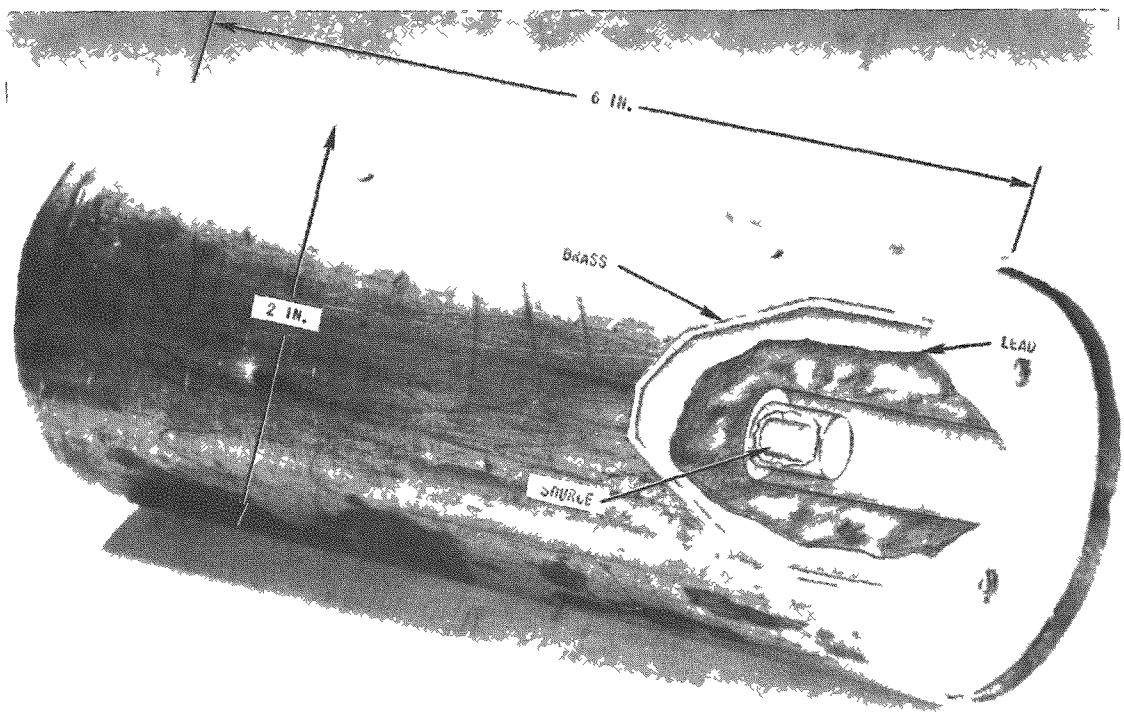

FIG. 3
SOURCE AND SHIELDING

B. Scintillation Crystal-Photomultiplier Tube Assembly

The scintillation crystal-photomultiplier tube assembly is shown in Fig. 4(a). The crystal is thallium-activated sodium iodide, $1\frac{1}{4}$ in. diameter by 1 in. thick. The photomultiplier tube is either an RCA-Type 5819 or a DuMont-Type 6292. The only special characteristic required of the photomultiplier tube is that it have a very low dark current (about 0.01×10^{-6} amp). Dark current refers to that current produced within the photomultiplier in the absence of light. This dark current arises from two major causes: (1) leakage paths from the high potentials on the photocathode and dynodes, and (2) from the thermionic emission of electrons from the photocathode and dynodes. The dark current of the tube sets a lower limit on the intensity of radiation that can be measured accurately. As thulium-170 has a rather short half-life, the radiation intensity of the source decreases after a short period to the point where this lower limit of accurate detection is approached unless the photomultiplier tube dark current is very low.

A Lucite light guide is affixed to the face of the tube for the purpose of optically coupling the tube to the scintillation crystal. The tube, light guide, and mu-metal shield are partially sealed in an aluminum can. The scintillation crystal is coupled to the light guide with silicone grease and the enclosure completed, making the entire assembly light tight.(5)

The scintillation crystal is protected from extraneous radiation by a lead shield (Fig. 4b) which surrounds the crystal and extends over part of the photomultiplier tube can. The rectangular window in the face of the shield is slightly greater than the width of the flow channel. Photographic film is inserted in the slot in the face of the shield to facilitate alignment of the window with the flow channel.

C. Magnetic Shielding

The face of the photomultiplier tube is located 5 in. from the flow channel which, at times, is heated by a maximum of 3,250 amp. Therefore, shielding is required to attenuate the magnetic field produced by the a-c currents so that the output current of the tube is essentially independent of this field. In addition to the mu-metal cylinder which surrounds the body of the tube. the external shielding includes three concentric mu-metal enclosures and a 0.25-in. thick annealed steel box.

D. Cooling System

Water cooling coils of copper tubing - one coil wrapped tightly around the tube can, and the other soldered to the magnetic shield - are used to maintain the photomultiplier tube at a fairly constant temperature of ~20°C. The cooling system reduces the temperature-sensitive drifts inherent in this type of tube and crystal, and protects the tube from the high ambient temperature surrounding the flow channel.

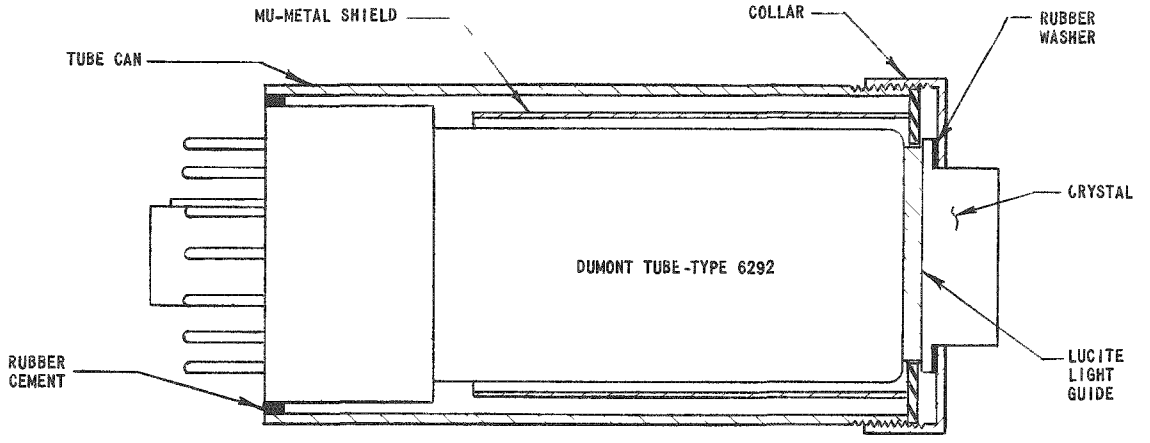

(A) TUBE-CRYSTAL COMPONENTS

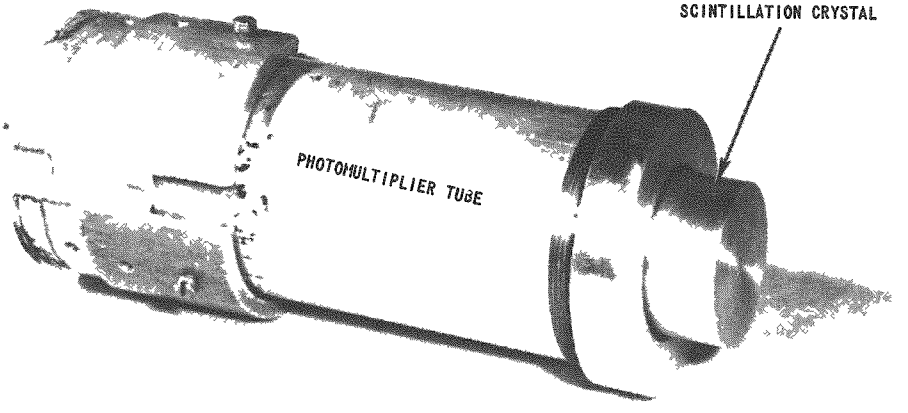

(B) FINAL ASSEMBLY WITH CRYSTAL SHIELDING REMOVED

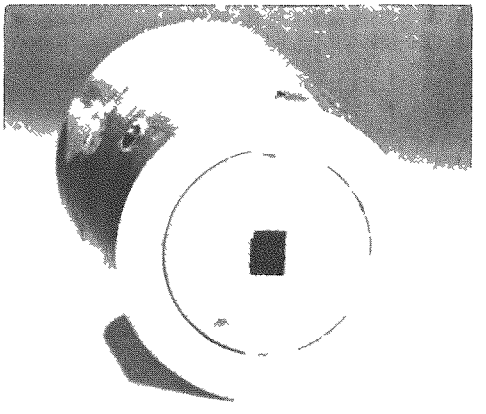

(C)
SCINTILLATION CRYSTAL SHIELD

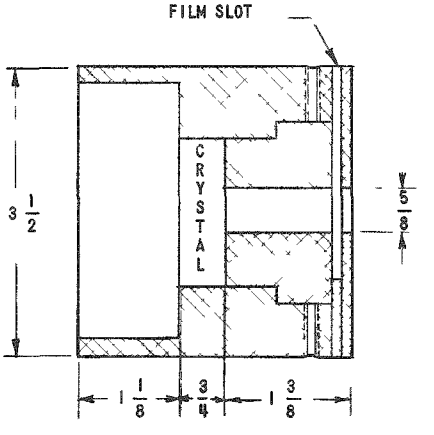

FIG. 4
SCINTILLATION CRYSTAL - PHOTOMULTIPLIER TUBE ASSEMBLY

E. Instrumentation

The instrumentation consists of a current amplifier and a negative high-voltage supply, and a d-c Esterline-Angus recorder (Fig. 5).

The photomultiplier tube output is fed to the current amplifier whose output voltage is proportional to the input current. The amplifier has full-scale input ranges of 1×10^{-8}, 5×10^{-8}, 2×10^{-7}, 1×10^{-6}, 5×10^{-6}, 2×10^{-5}, and 1×10^{-4} amp which, in turn, correspond to 10 volts output. The negative high-voltage supply is required for the photocathodes and dynodes of the photomultiplier tube. The supply is regulated to 0.1% to prevent large changes in tube gain.

The recorder has a range of 0 to 10 volts, and a pen swing time of 1 sec. This slow response effectively damps out many of the variations in voltage due to the statistical nature of the radiation being measured and aids in determining steady-state values. Recorders having faster response are available if transient measurements are desired.

F. Lucite Mock-Up of Preferential Phase Distributions

Under certain conditions in boiling channels, preferential phase distributions corresponding to various flow patterns are encountered in two-phase mixtures. For example: in the local boiling region of the channel (region of incipient boiling), it is believed that the steam bubbles form on the channel walls while the remaining volume of the channel is mostly water. In this case the steam-water mixture cannot be illustrated by layers of water and steam perpendicular to the incident radiation (see illustration, p. 4), and Eq. (15) no longer gives the true void fraction.

The deviations from the void-fraction equation (Eq. 15) produced by the preferential phase distributions were determined with the aid of the full-scale mock-up of the boiling channel shown in Fig. 6. The source and photomultiplier tube were positioned to duplicate the geometry of the radiation path. The flow patterns selected for study were constructed of Lucite because of its close similarity to water in density and absorption coefficient. The voids in the Lucite were simulated by machining predetermined geometric patterns to effect the corresponding phase distributions.

The Lucite blocks (Fig. 7) were placed in the mock-up channel and their respective void fractions determined with respect to (1) an empty channel; (2) an air-filled channel; and (3) a solid block of Lucite. The void fractions were then computed by Eq. (15) and compared with the measured values. The results of these tests are discussed in the following section.

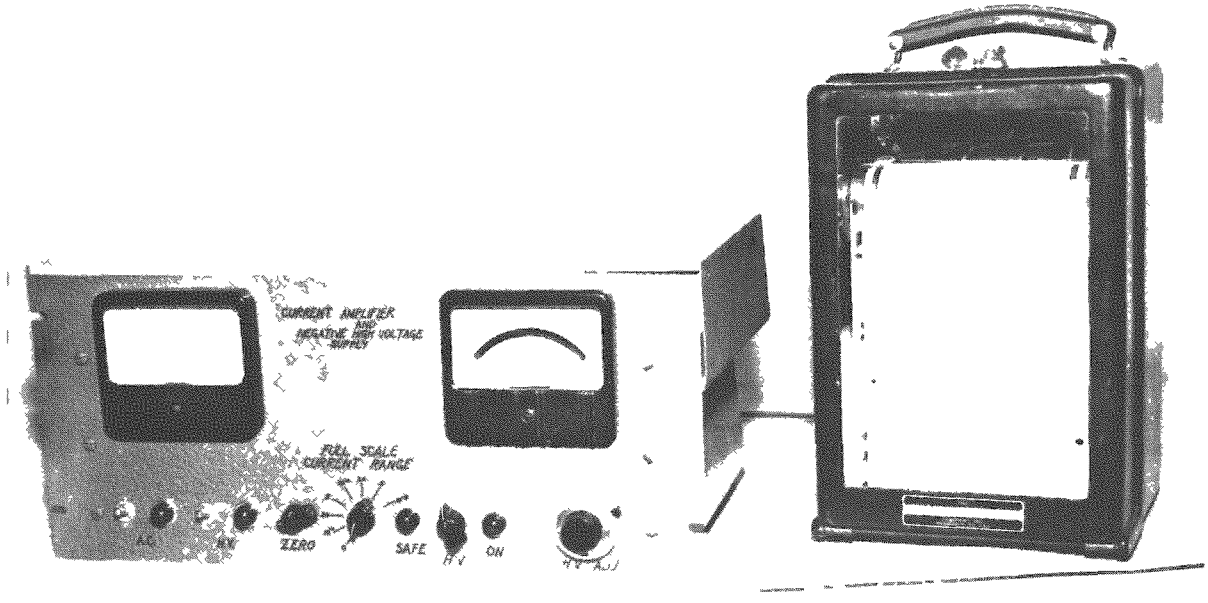

CURRENT AMPLIFIER AND NEGATIVE HIGH-VOLTAGE SUPPLY

RECORDER

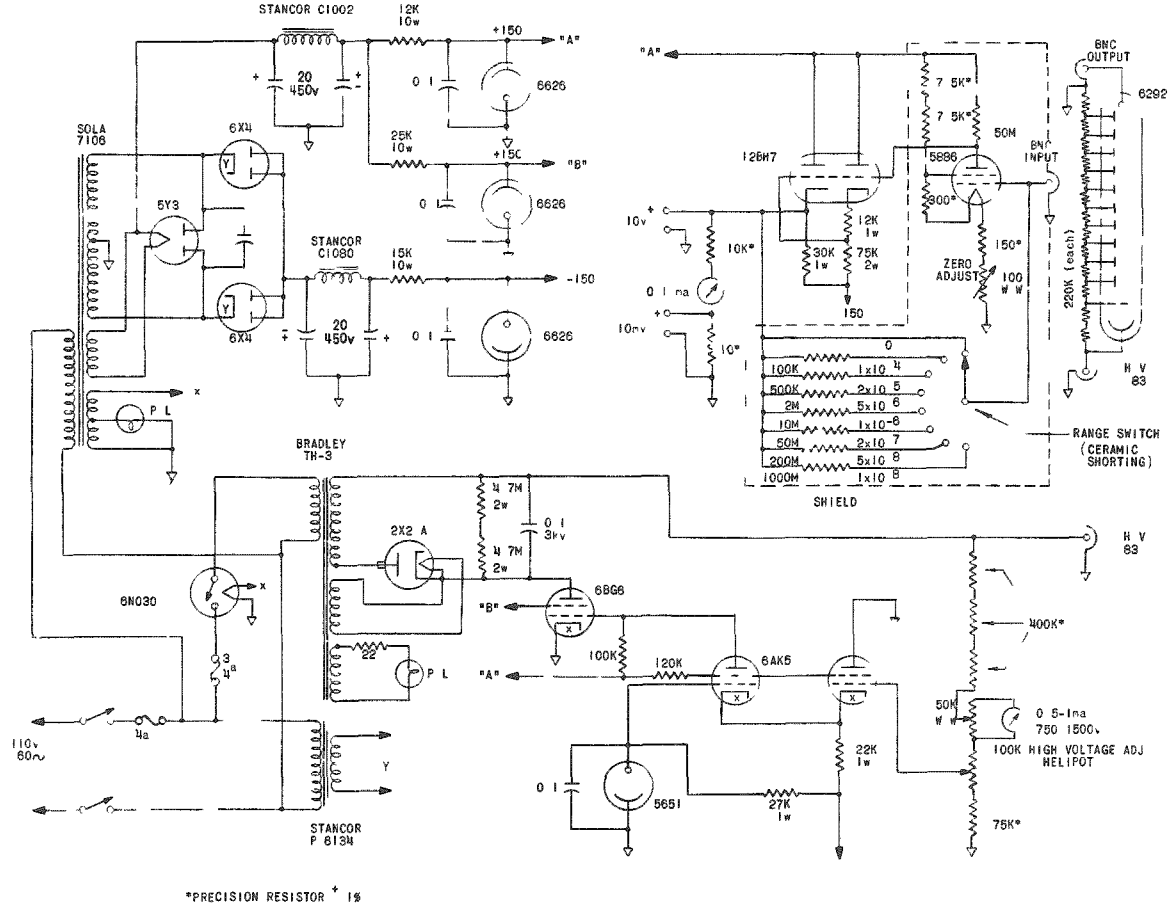

FIG 5

SYSTEM INSTRUMENTATION AND CIRCUITRY

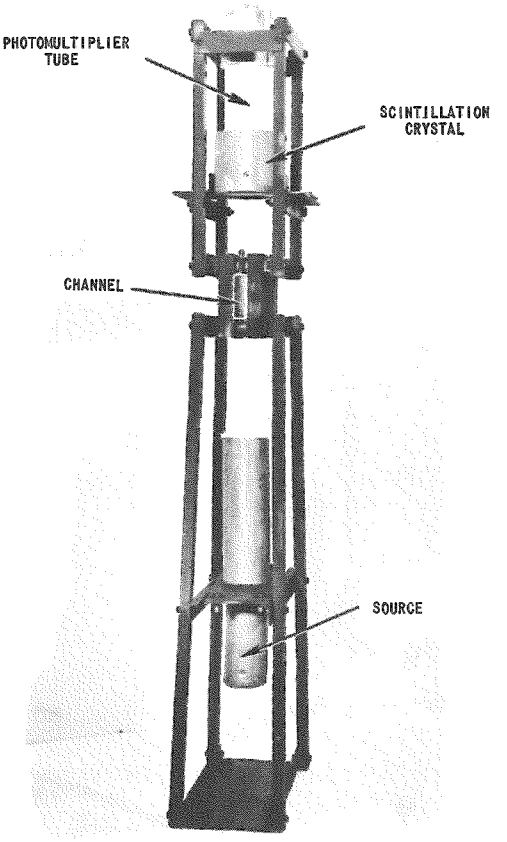

FIG. 6
ASSEMBLY USED TO STUDY PREFERENTIAL FLOW PATTERNS

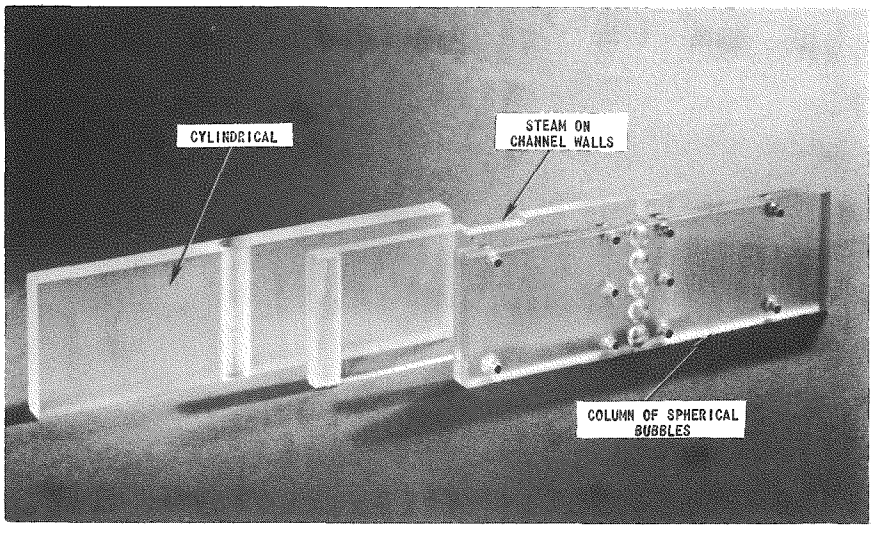

FIG. 7
LUCITE MOCK-UPS OF PREFERENTIAL FLOW PATTERNS

IV. ERROR ANALYSIS

Several sources of error inherent in the described method of measuring steam void fraction were analyzed to determine the over-all accuracy of the results obtained from both test facilities. The first group of errors includes those arising from the electronics of the system. The second group covers the sources of error in the measurement technique. The third group of errors points out the limitations of the system when preferential distribution patterns are encountered.

Provided the error is small, the per cent error in steam void fraction, α, for any source of error is

$$\% \text{ Error} = \left[\left(\frac{\partial \alpha}{\partial v}\right)\left(\frac{\Delta v}{\alpha}\right) + \left(\frac{\partial \alpha}{\partial v_f}\right)\left(\frac{\Delta v_f}{\alpha}\right) + \left(\frac{\partial \alpha}{\partial v_e}\right)\left(\frac{\Delta v_e}{\alpha}\right)\right](100) \quad . \tag{16}$$

where α is given by Eq (15) and Δv, Δv_f, Δv_e are absolute errors of the indicated quantities.

From Eq. (15)

$$\frac{\partial \alpha}{\partial v} = \frac{1}{v \ln\left(\frac{v_e}{v_f}\right)} \tag{17}$$

$$\frac{\partial \alpha}{\partial v_f} = -\frac{\ln\left(\frac{v_e}{v}\right)}{v_f\left[\ln\left(\frac{v_e}{v_f}\right)\right]^2} \tag{18}$$

$$\frac{\partial \alpha}{\partial v_e} = -\frac{\ln\left(v/v_f\right)}{v_e\left[\ln\left(v_e/v_f\right)\right]^2} \tag{19}$$

Substitution of Eqs. (17), (18), and (19) into Eq. (16) gives

$$\% \text{ Error} = \left[\frac{\Delta v}{\alpha v \ln\left(\frac{v_e}{v_f}\right)} - \frac{\left(\Delta v_f\right)\ln\left(\frac{v_e}{v}\right)}{\alpha v_f\left[\ln\left(\frac{v_e}{v_f}\right)\right]^2} - \frac{\left(\Delta v_e\right)\left[\ln\left(\frac{v}{v_f}\right)\right]}{\alpha v_e\left[\ln\left(\frac{v_e}{v_f}\right)\right]^2}\right](100) \tag{20}$$

Substitution for α in Eq. (20) yields

$$\% \text{ Error} = \left[\left(\frac{\Delta v}{v}\right)\ln\left(\frac{v_e}{v_f}\right) - \left(\frac{\Delta v_f}{v_f}\right)\ln\left(\frac{v_e}{v}\right) - \left(\frac{\Delta v_e}{v_e}\right)\ln\left(\frac{v}{v_f}\right)\right]\left[\frac{100}{\ln\left(\frac{v_e}{v_f}\right)\ln\left(\frac{v}{v_f}\right)}\right] . \tag{21}$$

Let

$$a = \frac{v_e}{v_f} \tag{22}$$

and

$$b = v_f \quad . \tag{23}$$

Then from Eq. (13),

$$v = b(a)^{\alpha} \quad . \tag{24}$$

Upon substituting Eqs. (22), (23) and (24) into Eq. (21), there is obtained

$$\% \text{ Error} = \left[\left(\frac{\Delta v}{v}\right) \ell n\,(a) - \left(\frac{\Delta v_f}{v_f}\right) \ell n\,(a)^{1-\alpha} \left(\frac{\Delta v_e}{v_e}\right) \ell n\,(a)^{\alpha}\right] \left[\frac{100}{\ell n\,(a)\ \ell n\,(a)^{\alpha}}\right] \quad . \tag{25}$$

For given errors, Δv, Δv_f, and Δv_e, the maximum per cent error is

$$\% \text{ Error} = \left[\left(\frac{\Delta v}{v}\right) \ell n\,(a) + \left(\frac{\Delta v_f}{v_f}\right) \ell n\,(a)^{1-\alpha} + \left(\frac{\Delta v_e}{v_e}\right) \ell n\,(a)^{\alpha}\right] \left[\frac{100}{\ell n\,(a)\ \ell n\,(a)^{\alpha}}\right] \tag{26}$$

If all voltage measurements are in error by the same percentage, or

$$\left(\frac{\Delta v}{v}\right)(100) = \left(\frac{\Delta v_f}{v_f}\right)(100) = \left(\frac{\Delta v_e}{v_e}\right)(100) = K \quad ,$$

the maximum per cent error becomes,

$$\% \text{ Error} = \left[\frac{K}{\ell n\,(a)\ \ell n\,(a)^{\alpha}}\right] \left[\ell n\,(a)^2\right] = \frac{2K}{\alpha\, \ell n\,(a)} \quad . \tag{27}$$

If all voltage measurements are in error by a certain per cent of full-scale voltage, or

$$\left(\frac{\Delta v}{v_{fs}}\right)(100) = \left(\frac{\Delta v_f}{v_{fs}}\right)(100) = \left(\frac{\Delta v_e}{v_{fs}}\right)(100) = C \quad ,$$

where v_{fs} represents the full-scale voltage, the maximum per cent error becomes

$$\% \text{ Error} = \left[\frac{v_{fs}\, C}{\alpha\, b\, \ell n\,(a)}\right] \left[a^{-\alpha} + 1 - \alpha + \frac{\alpha}{a}\right] = \left[\frac{v_{fs}\, C}{\alpha b\, \ell n\,(a)}\right] \left[a^{-\alpha} + 1 + \alpha \left(\frac{1}{a} - 1\right)\right] \quad . \tag{28}$$

The probable percentage error in α is, for any source of error,

$$\% \text{ P.E.} = \sqrt{\left(\frac{\partial \alpha}{\partial v}\right)^2 \left(\frac{\Delta v}{\alpha}\right)^2 + \left(\frac{\partial \alpha}{\partial v_f}\right)^2 \left(\frac{\Delta v_f}{\alpha}\right)^2 + \left(\frac{\partial \alpha}{\partial v_e}\right)^2 \left(\frac{\Delta v_e}{\alpha}\right)^2} \; (100) \quad . \qquad (29)$$

Substitution of Eqs. (17), (18), (19) and (15) into Eq. (29) gives

$$\% \text{ P.E.} = \sqrt{\left(\frac{\Delta v}{v}\right)^2 \left[\frac{1}{\ell n \left(\frac{v}{v_f}\right)}\right]^2 + \left(\frac{\Delta v_f}{v_f}\right)^2 \left[\frac{\left[\ell n \left(\frac{v_e}{v}\right)\right]^2}{\left[\ell n \left(\frac{v_e}{v_f}\right)\right]^2 \left[\ell n \left(\frac{v}{v_f}\right)\right]^2}\right] + \left(\frac{\Delta v_e}{v_e}\right)^2 \left[\frac{1}{\ell n \left(\frac{v_e}{v_f}\right)}\right]^2} \; (100) \quad . \qquad (30)$$

Substitution of Eqs. (22), (23), and (24) into Eq. (30) yields

$$\% \text{ P.E.} = \left[\frac{100}{\ell n\,(a)\,\ell n\,(a)^{\alpha}}\right] \sqrt{\left(\frac{\Delta v}{v}\right)^2 [\ell n\,(a)]^2 + \left(\frac{\Delta v_f}{v_f}\right)^2 [(\ell n\, a)^{1-\alpha}]^2 + \left(\frac{\Delta v_e}{v_e}\right)^2 [(\ell n\, a)^{\alpha}]^2} \qquad (31)$$

If all voltage measurements are in error by the same percentage, or

$$\left(\frac{\Delta v}{v}\right)(100) = \left(\frac{\Delta v_f}{v_f}\right)(100) = \left(\frac{\Delta v_e}{v_e}\right)(100) = K' \quad ,$$

where K' is the probable percentage error in the reading, then

$$\% \text{ P.E.} = \left[\frac{K'}{\ell n\,(a)\;\ell n\,(a)^{\alpha}}\right] \sqrt{[\ell n\,(a)]^2 + [\ell n\,(a)^{1-\alpha}]^2 + [\ell n\,(a)^{\alpha}]^2}$$

$$= \left[\frac{-K}{(\alpha)\;\ell n\,(a)}\right] \sqrt{2[1 - \alpha + (\alpha)^2]} \quad . \qquad (32)$$

For errors which are a percentage of full scale, or

$$\left(\frac{\Delta v}{v_{fs}}\right)(100) = \left(\frac{\Delta v_f}{v_{fs}}\right)(100) = \left(\frac{\Delta v_e}{v_{fs}}\right)(100) = C' \quad ,$$

where C' is the probable percentage error in the reading, then

$$\% \text{ P. E.} = \left[\frac{v_{fs}\, C'}{b\, \ell n\,(a)\, \ell n\,(a)^{\alpha}}\right] \sqrt{\frac{[\ell n\,(a)]}{(a)^{2\alpha}} + [\ell n\,(a)^{1-\alpha}]^2 + \frac{[\ell n\,(a)^{\alpha}]^2}{(a)^2}}$$

$$= \left[\frac{v_{fs}\, C'}{\alpha b\, \ell n\,(a)}\right] \sqrt{(a)^{-2\alpha} + (1-\alpha)^2 + (\alpha)^2\,(\alpha)^{-2}} \quad . \tag{33}$$

A. Errors in Electronics System

One source of error in the electronics of the system is the transfer characteristic of the amplifier, k_s. This constant was found to vary 0.5% of full scale for an 18-hr period without zero adjustment. The zero drift, which is a part of the transfer characteristic, was also found to vary 0.5% of full scale in 18 hr. Therefore, the changes in the transfer characteristic were primarily due to zero drift. As the zero is adjusted prior to each measurement, this source of error is essentially eliminated.

Another source of error is the variation in gain of the photomultiplier tube with variations of its supply voltage, v_h. As photomultiplier tube gain changes as the seventh power of v_h, for small variations in v_h, the error from these variations is seven times the regulation of the supply voltage. The regulation of the supply voltage was measured to be within 0.1%, or a maximum error of (7) (± 0.05%) or ±0.35%. Figure 8 shows the maximum per cent error calculated by Eq. (27), and the probable per cent error in α calculated by Eq. (32) for typical values of a and b obtained in the test facilities.

The third source of error is the reduction in gain of the crystal-tube assembly with increasing temperature. The average temperature coefficient of the assembly was measured to be -0.19%/°F over the range from 62 to 110°F.[3] As cooling coils are utilized, the maximum variation in temperature of the assembly was measured to be ± 2°F, or a maximum error of ± 0.38%. Figure 9 shows the maximum error calculated by Eq. (27), and the probable error in α calculated by Eq. (32) for typical values of a and b.

B. Errors in Measuring Technique

One source of error exists when a fixed amount of radiation reaches the detector by "parallel paths" external to the steam-water mixture. If the fixed amount of radiation is such that every measurement (v, v_f, v_e) is increased by a constant value Δv_1, then the per cent error in α is calculated by Eq. (25). If Δv_1 is small, where $C = \Delta v_1 / v_{fs}$, then

$$\% \text{ Error} = \frac{v_{fs}\, C \left[(a)^{-\alpha} - 1 + \alpha\left(1 - \frac{1}{a}\right)\right]}{\alpha\, b\, \ell n\,(a)}. \tag{34}$$

For $\alpha = 0$, Eq. (34) is indeterminate. Therefore, at $\alpha = 0$,

$$\% \text{ Error} = v_{fs}\, C \left[\frac{1 - \frac{1}{a} - \ell n\,(a)}{b\, \ell n\,(a)}\right]. \tag{35}$$

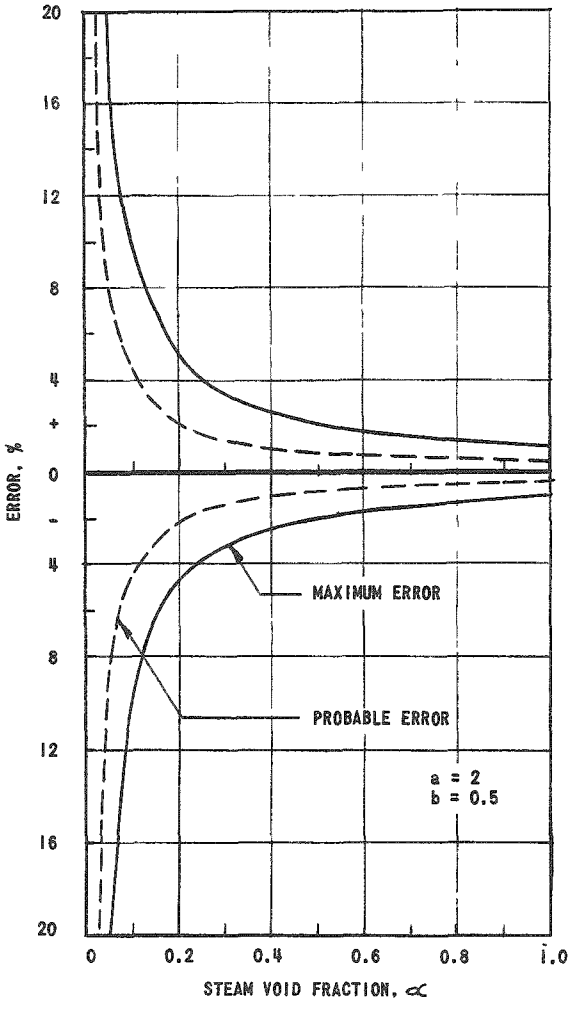

FIG. 8
PER CENT ERROR IN ∝ DUE TO HIGH VOLTAGE SUPPLY FLUCTUATIONS OF ±0.05%

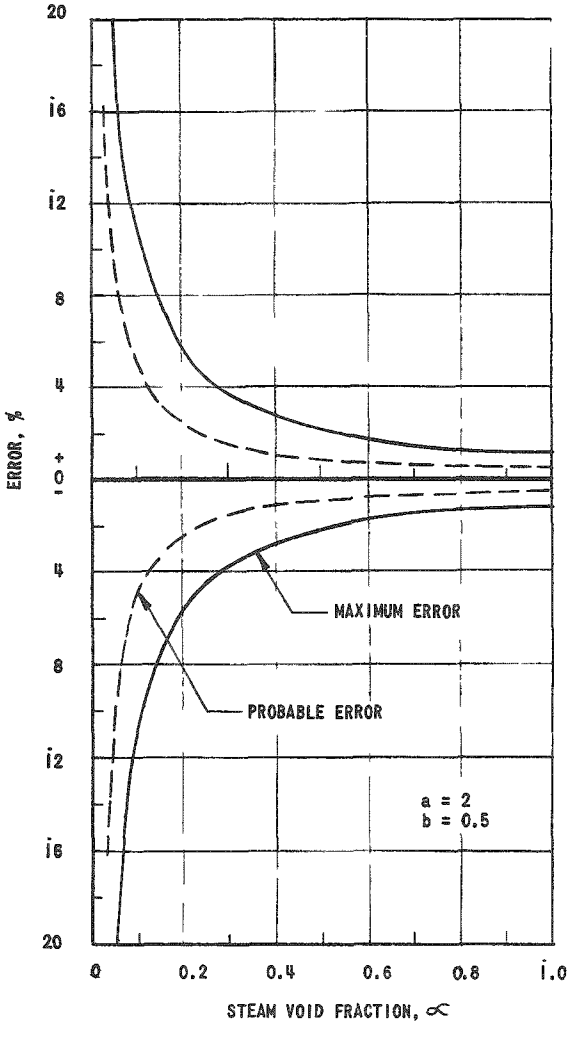

FIG. 9
PER CENT ERROR IN ∝ DUE TO TEMPERATURE VARIATIONS OF ± 2°F IN PM TUBE-SCINTILLATION CRYSTAL ASSEMBLY

If a large fixed amount of radiation reaches the detector by some parallel path so that every measurement of v is increased by a constant value, Δv, then

$$\alpha' = \frac{\ell n\ (v'/v'_f)}{\ell n\ (v'_e/v'f)} \quad , \tag{36}$$

where the primes indicate apparent values. Consequently,

$$\alpha' = \frac{\ell n\ [(v + \Delta v_1)/(v_f + \Delta v_1)]}{\ell n [(v_e + \Delta v_1)/(v_f + \Delta v_1)]} \quad , \tag{37}$$

where

Δv_1 = the increment in v due to the parallel paths of radiation.

Letting

$$\frac{v_e}{v_f} = a = \text{empty-to-full ratio,}$$

or

$$v_e = a\ v_f$$

and

$$\Delta v_1 = k v_f \quad ,$$

it follows from Eq. (13) that

$$v = v_f\ a^{\alpha} \quad . \tag{38}$$

Substituting these values in Eq. (19) yields

$$\alpha' = \frac{\ell n\ [(v_f\ a^{\alpha} + k v_f)/(v_f + k v_f)]}{\ell n\ [(a\ v_f + k v_f)/(v_f + k v_f)]}$$

or

$$\alpha' = \frac{\ell n\ [(a^{\alpha} + k)/(1 + k)]}{\ell n\ [(a + k)/(1 + k)]} \quad . \tag{39}$$

The per cent error in α is:

$$\% \text{ Error} = \left(\frac{\alpha'}{\alpha} - 1\right)(100)$$

$$= \left[\frac{\ell n\ [(a^{\alpha} + k)/(1 + k)]}{\alpha\ \ell n\ [(a + k)/(1 + k)]} - 1\right](100) \quad . \tag{40}$$

For $\alpha = 0$, Eq. (40) is indeterminate. Therefore, at $\alpha = 0$,

$$\% \text{ Error} = \left[\frac{\ell n\,(a)}{(1 + k)\,\ell n\,[(a + k)/(1 + k)]} - 1 \right] (100) \quad . \tag{41}$$

In Fig. 10, the per cent error is plotted as a function of α for two pairs of values of a and k. The error in void fraction is relatively small even when a substantial fraction of the total radiation arrives at the detector via fixed parallel paths.

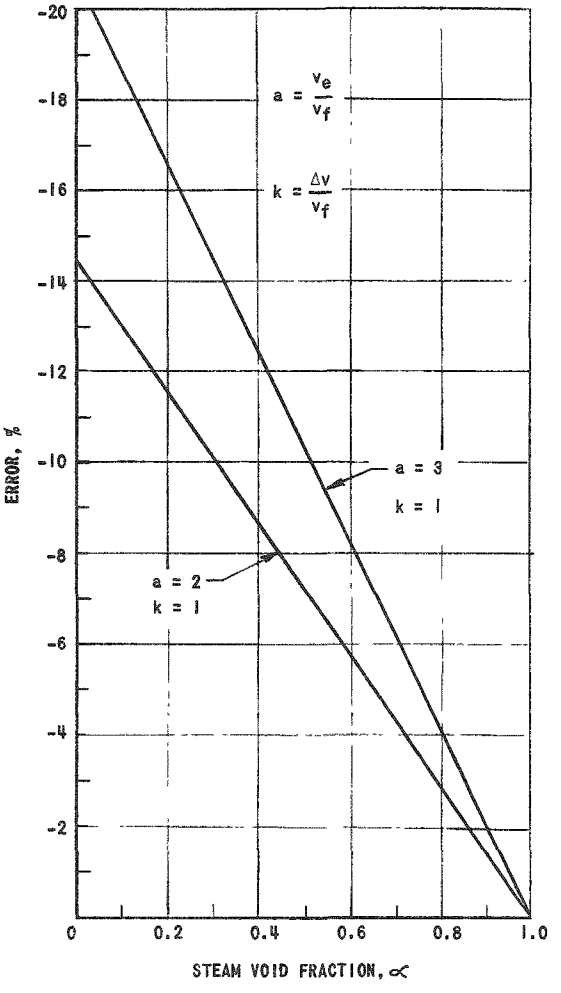

FIG. 10

PER CENT ERROR IN α DUE TO LARGE PARALLEL PATHS EXTERNAL TO THE HEATED CHANNEL

On the test facilities, the window in the scintillation crystal shield is made slightly larger than the channel width to facilitate alignment of the window with the channel. As the material external to the test section is steel and the window width and channel width are known, the flux reaching

the detector by "parallel paths" can be calculated for a particular test facility:

$$\Phi_p = A_p I_0 \exp(-\mu_p x_p) \tag{42}$$

$$\Phi_f = A I_0 \exp(-\mu_2 x) \tag{43}$$

where

Φ_p = the flux reaching the detector by some "parallel paths"

Φ_f = the flux reaching the detector through a channel filled with water

A_p = the area of the parallel path "seen" by the detector

μ_p = the absorption coefficient of the "parallel path" material

x_p = the thickness of the material in the "parallel path"

A = the area of the channel "seen" by the detector

μ_2 = the absorption coefficient of water

x = the distance through the water path.

Dividing Eq. (42) by Eq. (43),

$$\frac{\Phi_p}{\Phi_f} = \frac{A_p}{A} \exp(\mu_2 x - \mu_p x_p) \tag{44}$$

For a typical test facility:

$\mu_2 \approx 0.180$ per cm for water at 70F and for a radiation energy of 0.084 Mev.

$\mu_p \approx 3.93$ per cm for steel at 70F and for a radiation energy of 0.084 Mev.(6)

$x = x_p = 5.08$ cm

$A_p = 0.125$ in.^{2}.

$A = 0.5$ in.^{2}.

Therefore

$$\frac{\Phi_p}{\Phi_f} \approx (0.25) \exp\left\{(5.08)(-3.93)\right\}$$

$$= 6.25 \times 10^{-10}.$$

As Φ is proportioal to v,

$$v_p = (6.25 \times 10^{-10})\ (\Delta v_f) = \Delta v_1$$

and

$$C = \frac{\Delta v_1}{v_{fs}} \quad .$$

The per cent error in α caused by this "parallel path" is negligible.

Another source of error is the accuracy to which the strip chart recording voltmeter can be read. The maximum per cent error in α is obtained by Eq. (28) where

$$\left(\frac{\Delta v}{v_{fs}}\right)(100) = C$$

$$= \pm\ 0.125\% \quad ,$$

which is approximately the resolution of the scale on the Esterline Angus recorder. The probable per cent error in α is obtained from Eq. (33). The maximum and the probable per cent errors in α for inaccuracies in reading the strip chart are shown in Fig. 11 for a = 2 and b = 0.5.

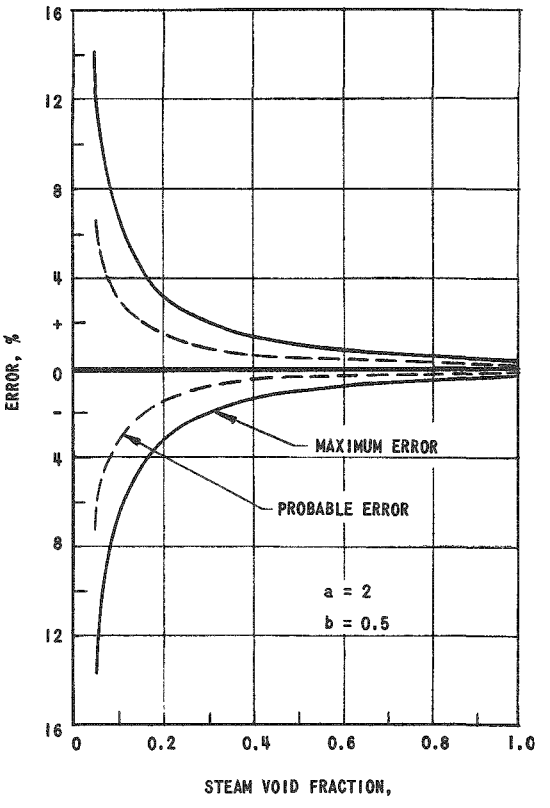

FIG. 11

PER CENT ERROR IN α DUE TO INACCURACIES OF ± 0.125% IN READING STRIP CHART

Consider now the effect of making the hot empty measurement at a pressure different from that of the void data runs to which it is applied. If in Eq. (3), x = 0, (α = 1), then

$$I_e = k_6 \exp(-\mu_3 x_0) \quad , \tag{45}$$

where:

I_e = the radiation intensity obtained with a steam-filled test section

$$k_6 = I_0 \exp(-\mu_1 d) \quad . \tag{46}$$

Since v is proportional to I, and if x = 0,

$$v_e = k_7 \exp(-\mu_3 x_0) \quad , \tag{47}$$

where

$$k_7 = \frac{v_e}{I_e} \quad k_6 \quad .$$

Similarly, letting x = x_0 (α = 0) in Eq. (3)

$$I_f = k_6 \left[\exp(-\mu_3 x_0)\right] \left[\exp\left\{x_0 (\mu_3 - \mu_2)\right\}\right], \tag{48}$$

from which it follows that

$$v_f = k_7 \exp(-\mu_2 x_0) \quad . \tag{49}$$

Assuming an erroneous attenuation coefficient, μ_3', the apparent hot empty value for v becomes

$$v_e' = k_7 \exp(-\mu_3' x_0) \quad , \tag{50}$$

where the primes indicate apparent values.

From Eqs. (47), (49), and (50), it follows that

$$\frac{v_e'}{v_f} = \exp\left\{(x_0)(\mu_2 - \mu_3')\right\} \tag{51}$$

and

$$\frac{v_e}{v_f} = \exp\left\{(x_0)(\mu_3 - \mu_2)\right\} \quad . \tag{52}$$

If the apparent void fraction is represented by α', where

$$\alpha' = \frac{\ell n\,(v/v_f)}{\ell n\,(v'_e/v_f)} \quad ,$$

and the true void fraction is represented by α, then the per cent error in α is given by

$$\% \text{ Error} = \left(\frac{\alpha'}{\alpha} - 1\right)(100) \tag{53}$$

or

$$\% \text{ Error} = \left[\frac{\ell n\,(v_e/v_f)}{\ell n\,(v'_e/v_f)} - 1\right](100) \quad . \tag{54}$$

Substitution of Eq. (51) and (52) into Eq. (54) yields

$$\% \text{ Error} = \left(\frac{\mu_2 - \mu_3}{\mu_2 - \mu'_3} - 1\right)(100) \quad . \tag{55}$$

The absorption coefficient for steam under the conditions employed is proportional to the density, so that

$$\% \text{ Error} = \left(\frac{\rho_2 - \rho_3}{\rho_2 - \rho'_3} - 1\right)(100) \quad , \tag{56}$$

where

ρ_2 = density of water at experimental temperature and pressure

ρ_3 = density of steam at experimental temperature and pressure

ρ'_3 = density of steam at some other temperature and/or pressure at which the "empty" reading is made.

Figure 12 (a) shows the per cent error in α for the case where experimental runs and hot "full" readings are made at some pressure and "empty" readings are made at atmospheric pressure with saturated steam filling the channel. The error can be eliminated by applying the corresponding correction factor plotted in Fig. 12 (b).

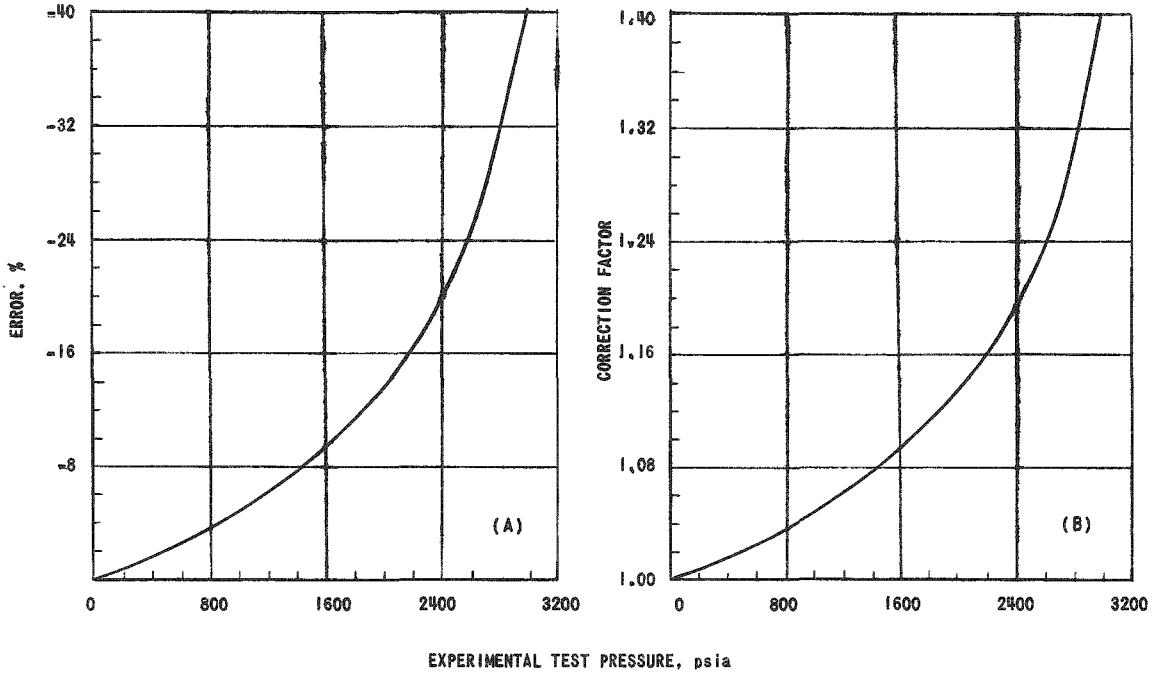

FIG. 12

(A) PER CENT ERROR IN α CAUSED BY TAKING "EMPTY" READING AT ATMOSPHERIC PRESSURE AND (B) CORRESPONDING CORRECTION FACTORS

C. Errors Arising from Decay of Radiation Source

Another source of error is the decay of the gamma-ray source over the period during which the tests are made. The error in the void fraction is determined by assuming the decay period to be 8 hr. The radiation intensity after time t is:

$$I_t = I_0 \exp(-\lambda t) \quad , \tag{57}$$

where

t = maximum time elapsed between the first and last readings

I_0 = initial intensity

λ = decay constant.

As the half-life of thulium is about 129 days, and $\lambda = 0.6931/T$, where T is the half-life in hours, there is obtained

$$\begin{aligned} I_t &= I_0 \exp\left[-(0.6931)(8)/(129)(24)\right] \\ &= I_0 \exp(-0.001789) \\ &= 0.9982\ (I_0) \quad . \end{aligned}$$

As I is proportional to v,

$$v_t = 0.9982\ (v)$$

and the error is a percentage of the reading, or

$$\left(\frac{\Delta v}{v}\right)(100) = -0.18\% \quad .$$

The maximum error will occur if a set of "full" readings is taken at the beginning of an 8-hour period, and the "empty" reading is taken at the conclusion of the same period. Under these conditions, and using Eq. (25) the per cent error in steam void fraction is constant and is only 0.26% for a = 2. This is considered negligible.

D. Errors Due to Preferential Phase Distributions

1. Calculated

As mentioned previously, Eq. (15) no longer gives the true steam void fraction when preferential phase distributions are encountered in boiling channels. The theoretical per cent error in the determination of steam void fraction for certain idealized phase distributions can be calculated by the equations derived in the Appendix. The three selected phase distributions are shown in Fig. 7.

a. Steam on Channel Walls

With steam present on all channel walls, and with a medium having an attenuation constant, μ, filling the remainder of the channel,

$$\alpha = \frac{x_c\, x_0 - x\, x_c - (x)^2 + x\, x_0}{x_c\, x_0} \tag{58}$$

By a method similar to that used to determine the effect of external parallel paths,

$$\frac{v'}{v_f} = \left(\frac{a}{h}\right)\left[\frac{1+h}{2} - \frac{\sqrt{(h+1)^2 - 4h\alpha}}{2} + \left\{\frac{h-1}{2} + \frac{\sqrt{(h+1)^2 - 4h\alpha}}{2}\right\}\right.$$

$$\left.\exp_a - \left\{(1 - h/2) + \sqrt{(h+1)^2 - 4h\alpha/2}\right\}\right] \quad , \tag{59}$$

where

$$a = \frac{v_e}{v_f}$$

$$h = \frac{x_c}{x_0}$$

v' = a measured voltage which is in error because of preferential phase distribution effects.

b. Cylindrical Steam Voids

Although the cylindrical steam void distribution does not represent a realistic two-phase distribution, it was selected because it could be readily checked with a Lucite mock-up. For this preferential phase distribution

$$\alpha = \frac{\pi r^2}{x_c x_w} \tag{60}$$

and

$$\frac{v'}{v_f} = 1 + \alpha (a - 1) \quad . \tag{61}$$

c. Columns of Spherical Bubbles

With columns of spherical bubbles in the channel

$$\alpha = \frac{4 \pi r^3 m n}{3 x_0 x_c x_w} \tag{62}$$

and

$$\frac{v'}{v_f} = 1 + \left[\frac{\pi m}{x_c x_w}\right] \left[\frac{\left\{(2nr/x_0) \ln(a) - 1\right\} \left\{\exp_a (2n r/x_0)\right\} + 1}{\left\{(2n^2)/x_0)^2\right\} [\ell n(a)]^2} - r^2\right] , \tag{63}$$

where

m = number of identical columns

n = number of bubbles per column

$a = \frac{v_e}{v_f}$

r = bubble radius.

For all three cases, the apparent void fraction may be expressed by

$$\alpha' = \frac{\ell n (v'/v_f)}{\ell n (v_e/v_f)} \quad . \tag{64}$$

2. Calculated vs Measured

The validity of the calculated void fractions was checked by measurements on Lucite mock-ups designed to simulate the three types of preferential phase distributions. The measured values include errors in the electronics system and measuring technique and indicate the maximum per cent error for a given preferential phase distribution.(7)

Figure 13 shows the calculated vs the measured per cent error in void fraction for the case of steam on the channel walls with values of h = 1/4 and a = 2. Figure 14 contains similar information for cylindrical voids where a = 2.

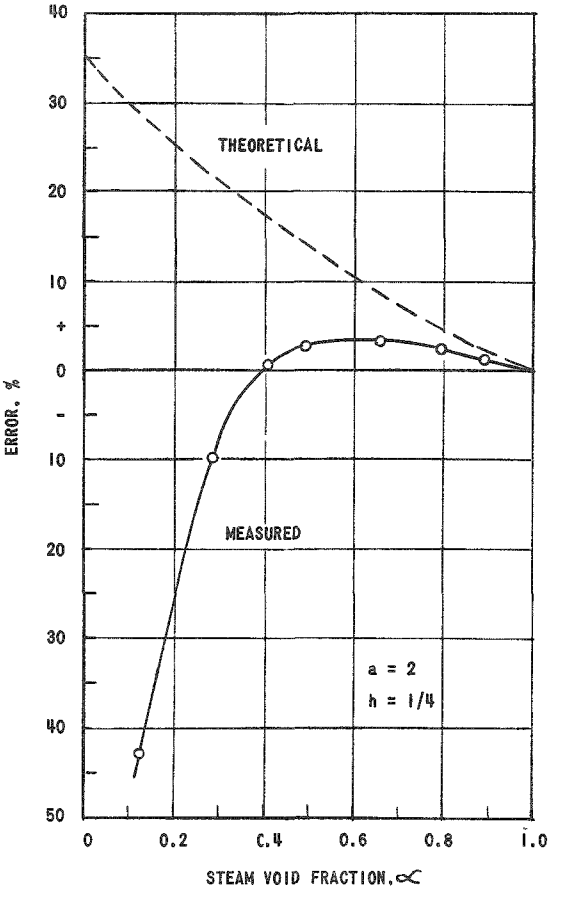

FIG. 13
MEASURED AND THEORETICAL PER CENT ERROR IN ∝ FOR PREFERENTIAL DISTRIBUTION OF STEAM ON CHANNEL WALLS

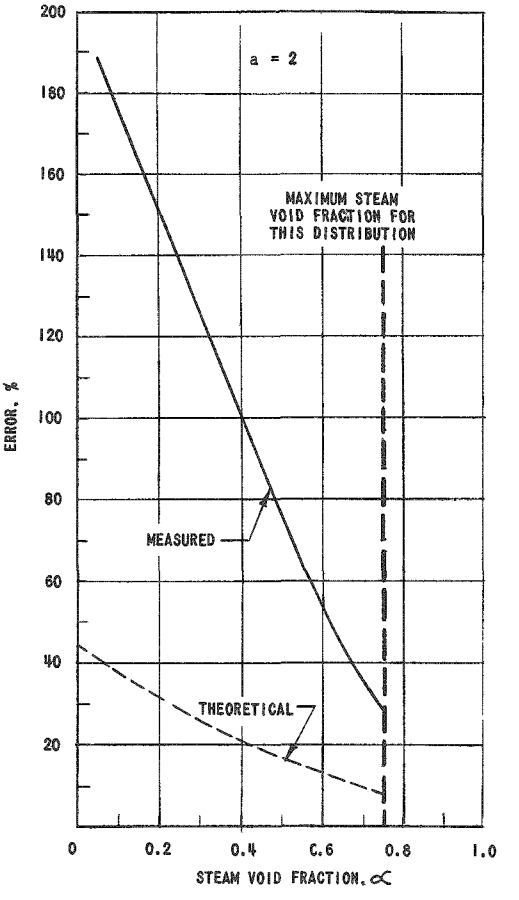

FIG. 14
MEASURED AND THEORETICAL PER CENT ERROR IN ∝ FOR PREFERENTIAL DISTRIBUTION OF CYLINDRICAL STEAM VOIDS IN THE CHANNEL

The Lucite model of the spherical void pattern contained a column of five bubbles, each 3/8 in. in diameter. The measured void fraction was 0.415. The theoretical void calculation indicated a value of 0.320. The actual void fraction was 0.281.

It is believed that the large discrepancy between the calculated and the measured errors with preferential phase distributions is due to an effect of geometry, such as non-uniformity of incident radiation. Studies are being made to resolve the discrepancies and to develop methods for eliminating the errors in the system.

E. Verification of Theory

The mock-up channel facility (Fig. 6) was also used to determine whether a truly exponential attenuation as a function of voids is obtained with layers of steam and water disposed perpendicular to the path of radiation. The test results indicated that, for all practical purposes, this relationship does exist.

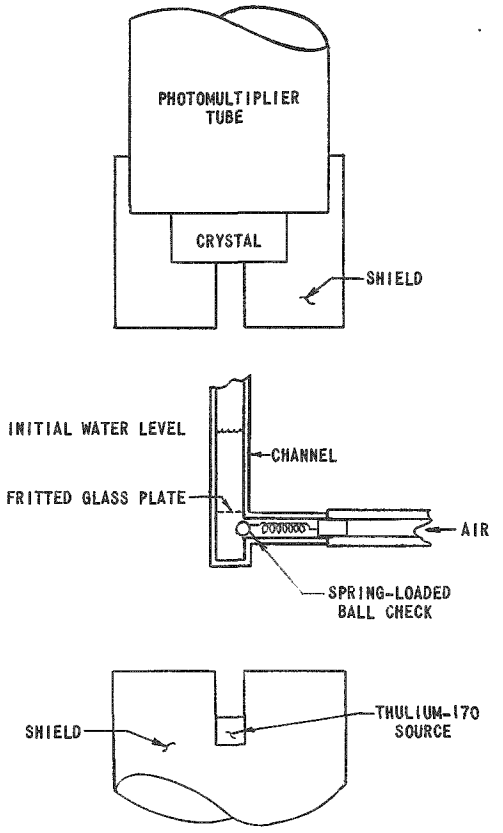

FIG. 15
SCHEMATIC OF HOMOGENEOUS MIXTURE TEST APPARATUS

Two series of tests were performed to verify the assumption that a homogeneous mixture of bubbles in water can be represented by alternate layers of steam and water arranged perpendicular to the incident radiation. The first series of tests were made on a mock-up channel filled with Lucite chips. Void fractions ranging from ~0.820 to 0.660 were simulated by compressing the mass of chips to various degrees. The results indicated errors well within the accuracy of the system.

The second series of tests was performed with air-water mixtures. The test equipment is shown schematically in Fig. 15. The channel was simulated by a square transparent container partially filled with water. The small bubbles were produced by

adding a small quantity of wetting agent to the water and by injecting air through the fritted glass plate near the bottom of the container. If the initial assumption is correct, no apparent change in density should be observed as air is bubbled through the water, because the total quantities of air and water in the path of radiation remain unchanged. The air, however, is now present as small bubbles in the channel and from all visual observations the mixture appeared to be homogeneous. Void fractions ranging from zero to 0.500 were studied. Again the results showed errors which were within the accuracy of the system.

IV. CONCLUSIONS

From the results of the error analysis it is apparent that there are several limitations on the ability of this system to accurately measure steam void fractions. The most important limitation is the loss of accuracy in the steam void fraction region below 0.100. For a uniform distribution of steam voids, the maximum probable per cent error in the region between 0.100 and 1.00 occurs with a void fraction of 0.100 and is ± 7.5% from all causes in the present system. The maximum per cent error for this region is ±29%. A plot of total per cent error in steam void fraction is shown in Fig. 16. The solid line is maximum per cent error and the dashed line is the probable per cent error for a = 2 and b = 0.5. It can be seen that a maximum absolute error of approximately ±0.029 is applicable over the full void range.

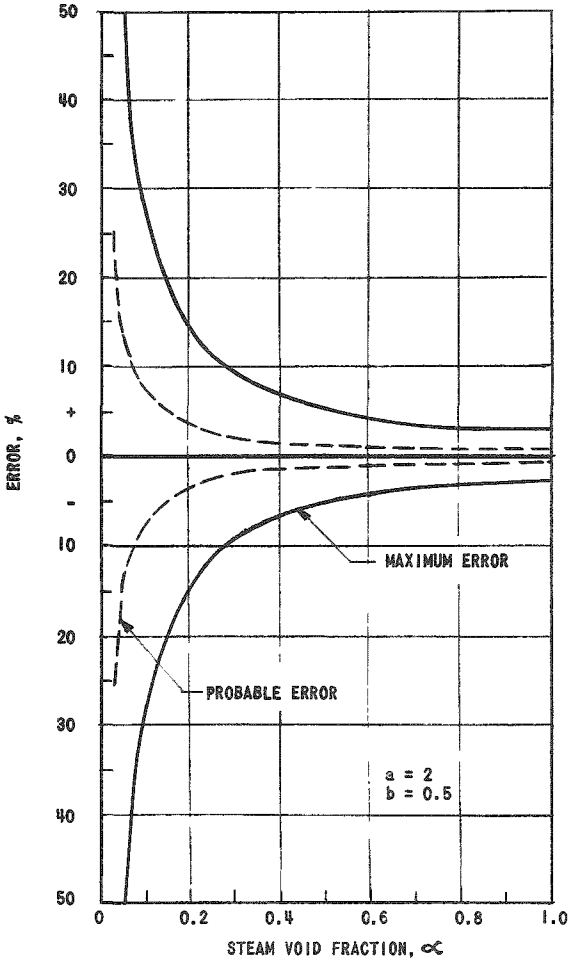

FIG. 16
TOTAL PER CENT ERROR IN ∝
FOR UNIFORM VOID DISTRIBUTION

The following measures should be taken to enhance the accuracy of the system:

(1) improve the regulation of the photomultiplier tube high-voltage supply;

(2) modify the tube-crystal cooling system to reduce temperature variations; and

(3) employ a more sensitive recorder.

When a non-uniform distribution of steam void fraction is known to exist, a system should be used wherein the portion of the channel being observed at any one instant is a small fraction of the total width of the channel. Thus the region examined becomes one having a more nearly uniform distribution of steam bubbles, with the consequent reduction of errors caused by the sensitivity of the system to preferential (non-uniform) void distributions. It follows that a curve of steam void fraction versus channel width can be drawn and the curve integrated to obtain the average steam void fraction. The results of preliminary tests based on this approach show a reduction by at least a factor of 2 in the errors arising from preferential phase distributions.[8,9]

APPENDIX

DERIVATION OF EQUATIONS FOR THEORETICAL PER CENT ERROR IN STEAM VOID FRACTION FOR IDEALIZED PHASE DISTRIBUTIONS

LOCAL BOILING DISTRIBUTION

With reference to the illustration, the light area denotes steam present on all channel walls and the cross hatching a medium having a linear absorption coefficient, μ.

By definition,

$$\alpha = \frac{x_c\, x_0 - x_c - x^2 + x\, x_0}{x_c\, x_0} \qquad (1)$$

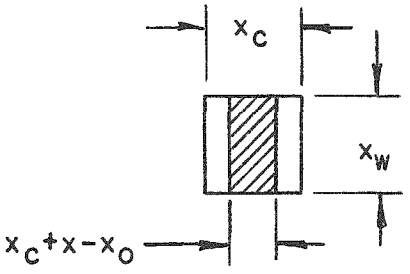

Rearrangement of terms leads to

$$x = \frac{x_0 - x_c + \sqrt{(x_c - x_0)^2 - 4\, x_0\, x_c(\alpha - 1)}}{2} . \qquad (2)$$

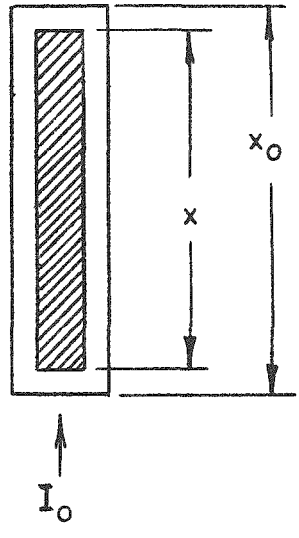

Now

$$\Phi_1 = [x_c - (x_c + x - x_0)]\, x_w\, I_0 = (x_0 - x)\, x_w\, I_0 \qquad (3)$$

$$\Phi_2 = (x_c + x - x_0)\, x_w\, I_0 \exp(-\mu x) \qquad (4)$$

$$\Phi_f = x_c\, x_w\, I_0 \exp(-\mu x_0) \qquad (5)$$

$$\Phi_e = x_c\, x_w\, I_0 \quad . \qquad (6)$$

The total flux is

$$\Phi_t = \Phi_1 + \Phi_2$$

and

$$\Phi' = (x_0 - x)\, x_w\, I_0 + (x_c + x - x_0)\, x_w\, I_0 \exp(-\mu x)$$

$$= x_c\, x_w\, I_0 \exp(-\mu x_0)$$

$$\left[\left(\frac{x_0 - x}{x_c}\right) \exp(\mu\, x_0) + \left(\frac{x_c + x - x_0}{x_c}\right) \exp\{-\mu\,(x - x_0)\}\right]$$

Division by Φ_f leads to

$$\frac{\Phi'}{\Phi_f} = \left(\frac{x_0 - x}{x_c}\right) \exp(\mu x_0) + \left(\frac{x_c + x - x_0}{x_c}\right) \exp\left\{-\mu (x - x_0)\right\} \quad . \tag{7}$$

Since v is proportional to Φ, and

$$\frac{v_e}{v_f} = \exp(\mu x_0) = a,$$

then

$$\frac{v}{v_f} = \frac{a(x_0 - x)}{x_c} + \frac{a(x_c + x - x_0)}{x_c} \exp(-\mu x)$$

$$= \frac{a}{x_c} \left[x_0 - x + (x_c + x - x_0) \exp_a (-x/x_0)\right] \quad . \tag{8}$$

Let

$$x_c = h x_0 \quad .$$

Then from Eq. (2)

$$x = \frac{x_0 (1 - h) + \sqrt{x_0^2 (h - 1)^2 - 4h (x_0)^2 (\alpha - 1)}}{2} \tag{9}$$

and

$$\frac{x}{x_0} = \frac{1 - h + \sqrt{(h + 1)^2 - 4 h \alpha}}{2} \quad . \tag{10}$$

Again, letting $x_c = h x_0$ in Eq. (8), and employing Eq. (10),

$$\frac{v'}{v_f} = \frac{a}{h} \left\{1 - \frac{1 - h + \sqrt{(h + 1)^2 - 4 h \alpha}}{2} +\right.$$

$$\left(h - 1 + \frac{1 - h + \sqrt{(h + 1)^2 - 4 h \alpha}}{2}\right)$$

$$\left.\exp_a - \left[\left\{1 - h + \sqrt{(h + 1)^2 - 4 h \alpha}\right\}/2\right]\right\}$$

$$= \frac{a}{h} \left\{\frac{1 + h}{2} - \frac{\sqrt{(h + 1)^2 - 4 h \alpha}}{2} + \left(\frac{h - 1}{2} + \frac{(h + 1)^2 - 4 h \alpha}{2}\right)\right.$$

$$\left.\exp_a - \left[\left\{1 - h + \sqrt{(h + 1)^2 - 4 h \alpha}\right\}/2\right]\right\} \quad . \tag{12}$$

From Eq. (64), p. 28,

$$\alpha' = \frac{\ell n\,(v'/v_f)}{\ell n\,(v_e/v_f)}$$

and

$$\left(\frac{\alpha'}{\alpha} - 1\right)\,(100) = \%\ \text{Error} \quad .$$

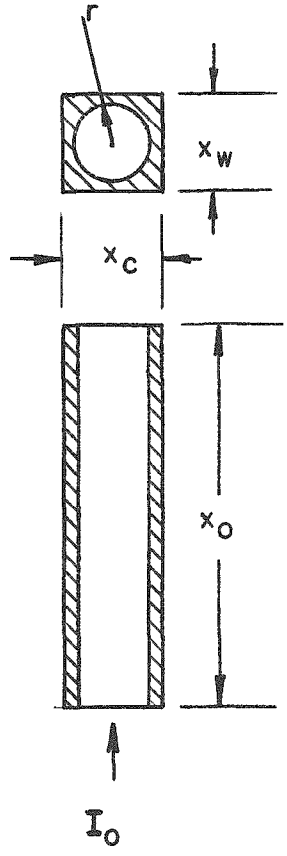

CYLINDRICAL STEAM VOIDS

With reference to the illustration:

$$\alpha = \frac{\pi\, r^2}{x_c\, x_w} \qquad (13)$$

$$\Phi_1 = I_0\,[x_0\, x_w - \pi\, r^2]\,\exp\,(-\mu x_0) \qquad (14)$$

$$\Phi_2 = I_0\,\pi\, r^2 \quad . \qquad (15)$$

Again,

$$\Phi_f = I_0\, x_c\, x_w \exp\,(-\mu x_0)$$

$$\Phi_e = I_0\, x_c\, x_w$$

$$\frac{\Phi_e}{\Phi_f} = \exp\,(\mu x_0) = a \quad . \qquad (16)$$

The total flux is

$$\Phi' = \Phi_1 + \Phi_2$$

$$= I_0\,[x_c\, x_w - \pi\, r^2]\,\exp\,(-\mu x_0) + I_0\,\pi\, r^2 \qquad (17)$$

$$\frac{\Phi'}{\Phi_f} = 1 - \frac{\pi\, r^2}{x_c\, x_w} + \frac{\pi\, r^2}{x_c\, x_w}\,\exp\,(\mu x_0)$$

$$= 1 - \frac{\pi\, r^2}{x_c\, x_w} + \frac{a\,\pi\, r^2}{x_c\, x_w} = 1 + (a - 1)\,(\alpha) \quad . \qquad (18)$$

Since v is proportional to Φ,

$$\frac{v'}{v_f} = 1 + (a - 1)\,(\alpha) \quad . \qquad (19)$$

Again from Eq. (64),

$$\alpha' = \frac{\ell n\ (v'/v_f)}{\ell n\ (v_e/v_f)}$$

and

$$\left(\frac{\alpha'}{\alpha} - 1\right)(100) = \%\ \text{Error}.$$

The limiting value of r is

$$r = \frac{x_c}{2} \text{ or } \frac{x_w}{2} \quad ,$$

depending on which is the smallest value. Therefore, the limiting value of α is

$$\alpha \leq \frac{\pi\ x_c}{4\ x_w} \text{ or } \frac{\pi\ x_w}{4\ x_c} \quad .$$

COLUMN OF SPHERICAL BUBBLES

The attenuation of a cylinder containing one bubble is determined initially. With reference to the illustration,

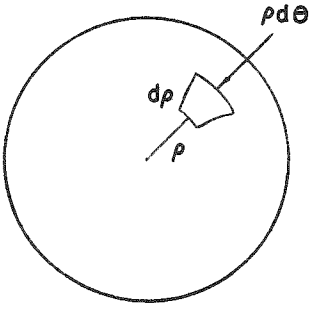

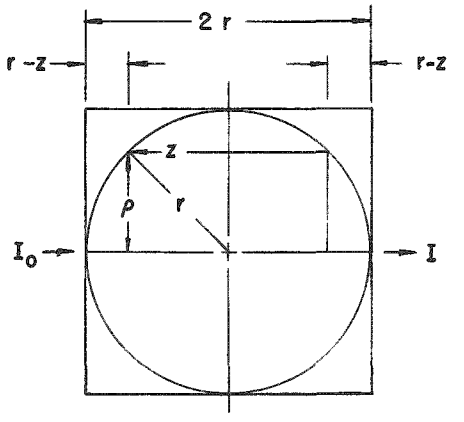

$$\rho^2 + z^2 = r^2 \tag{20}$$

$$z = r^2 - \rho^2 \tag{21}$$

$$d\Phi_1 = I_0\ \rho d\rho\ d\theta\ \exp\left\{-\ 2\mu\ (r - z)\right\} \quad . \tag{22}$$

$$\Phi_1 = I_0 \exp(-2\mu r) \int_0^r \exp(2\mu z)\, \rho d\rho \int_0^{2\pi} d\theta$$

$$= 2\pi I_0 \exp(-2\mu r) \int_0^r \exp(2\mu z)\, \rho d\rho \tag{23}$$

$$\rho d\rho = -z dz \tag{24}$$

when $\rho = 0$, $z = r$

and when

$$\rho = r, \; z = 0$$

$$\Phi_1 = 2\pi I_0 \exp(-2\mu r) \int_r^0 \exp(2\mu z)\, z dz$$

$$= 2\pi I_0 \exp(-2\mu r) \int_0^r z \exp(-2\mu z)\, dz \tag{25}$$

$$= 2\pi I_0 \exp(-2\mu r) \left[\frac{\exp(2\mu z)}{4\mu^2} (2\mu z - 1) \right]_0^r \tag{26}$$

$$= \pi I_0 \exp(-2\mu r) \left[\frac{(2\mu r - 1) \exp(2\mu r) + 1}{2\mu^2} \right]$$

$$= \left[\frac{\pi I_0}{2\mu^2} \right] [2\mu r - 1 + \exp(-2\mu r)] \; . \tag{27}$$

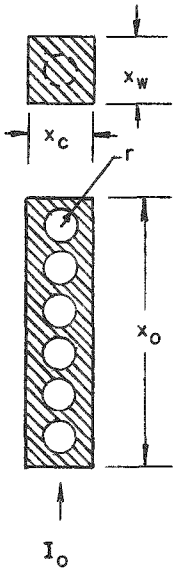

For n cylinders stacked vertically (see illustration),

$$\Phi_1 = 2\pi I_0 \exp(-2n\mu r) \left[\frac{(2n\mu z - 1) \exp(2n\mu z)}{4n^2\mu^2} \right]_0^r \tag{28}$$

$$= \left[\frac{(\pi)(I_0)}{(2)(n^2)(\mu^2)} \right] [(2)(n)(\mu)(r) - 1 + \exp(-2n\mu r)] \; . \tag{29}$$

Let the total path length equal $x_0 > 2nr$. Then a cylindrical path remains, having a depth

$$x = x_0 - 2nr \; . \tag{30}$$

The attenuation with this cylinder is

$$\Phi_1' = \Phi_1 \exp \left\{-\mu(x_0 - 2\,n\,r)\right\}$$

$$= \frac{\pi I_0 \exp(-\mu x_0)}{2\,n^2\,\mu^2}\left[(2\,n\mu r - 1)\exp(2\,n\mu r) + 1\right] \quad . \tag{31}$$

For m identical columns of spherical bubbles,

$$\Phi_m = m\Phi_1'$$

$$= \frac{m\,\pi\,I_0 \exp(-\mu x_0)}{2\,n^2\,\mu^2}\left[(2\,n\mu r - 1)\exp(2\,n\mu r) + 1\right] \quad . \tag{32}$$

If the total area examined is

$$A = x_c\,x_w \quad ,$$

and the projected area of m columns of bubbles is

$$m\,\pi\,r^2 \quad ,$$

the area devoid of bubbles is

$$A - m\,\pi\,r^2 = x_c\,x_w - m\,\pi\,r^2 \quad .$$

The flux received from the area $x_c\,x_w - m\,\pi\,r^2$ is

$$\Phi_2 = I_0\left[x_c\,x_w - m\,\pi\,r^2\right]\exp(-\mu x_0) \quad . \tag{33}$$

The total flux reaching the detector is

$$\Phi' = \Phi_m + \Phi_2$$

$$= I_0 \exp(-\mu x_0)\left[x_c\,x_w\,m\pi\left[\frac{(2\,n\mu r - 1)\exp(2\,n\mu r) + 1}{2\,n^2\,\mu^2} - r^2\right]\right] \quad . \tag{34}$$

Now again

$$\Phi_f = I_0\,x_c\,x_w \exp(-\mu x_0)$$

$$\Phi_e = I_0\,x_c\,x_w \quad .$$

From Eq. (16)

$$\mu = \frac{\ell n\,(a)}{x_0} \quad . \tag{35}$$

Then

$$\exp\,(2\,n\mu r) = \exp\,[(2\,n\,r/x_0)\,\ell n\,(a)]$$

$$= \exp_a\,(2\,n\,r/x_0) \qquad (36)$$

Substituting Eqs (35) and (36) in Eq (34) and dividing by Φ_f

$$\frac{\Phi'}{\Phi_f} = 1 + \left[\frac{m\pi}{x_c\,x_w}\right]\left[\frac{\left\{(2\,n\,r/x_0)\,(\ell n\,a) - 1\right\}\left\{\exp_a\,(2\,n\,r/x_0)\right\} + 1}{(2\,n^2)/(x_0)^2\,[\ell n\,(a)]^2} - r^2\right] \qquad (37)$$

As Φ is proportional to v

$$\frac{\Phi'}{\Phi_f} = \frac{v'}{v_f} \qquad (38)$$

From Eq. (64)

$$\alpha' = \frac{\ell n\,(v'/v_f)}{\ell n\,(v_e/v_f)}$$

By definition

$$\alpha = \frac{4\,\pi\,r^3\,n\,m}{3\,x_c\,x_w\,x_0}$$

and

$$\text{Error} = \left(\frac{\alpha'}{\alpha} - 1\right)\,(100)$$

REFERENCES

1. R. K. Swank, "Characteristics of Scintillators," Ann. Rev. Nucl. Sci. 4, 114 (1954).

2. W. P. Ball, R. Booth and M. H. MacGregor, "Scintillator Temperature Coefficients," Abstracts of the American Physical Society Meeting at Washington, D.C. (April, 1956), Series II, Vol. 1, No. 4.

3. F. W. Kinard, "Temperature Dependence of Photomultiplier Tube Gain," Nucleonics, Vol. 15 (No. 4), 92 (1957).

4. R. L. Graham, J. L. Wolfson, and R. E. Bell, "The Disintegration of Tm^{170}," Can. J. Phys. 30, 459 (1952).

5. R. K. Swank and J. S. Moenich, "Potting of Photomultiplier Tubes," ANL-5239 (February, 1954).

6. Gladys White Grodstein, "X-Ray Attenuation Coefficients from 10 kev to 100 Mev," National Bureau of Standards, C-583 (April, 1957).

7. R. R. Rhode and W. H. Cook, "Effect of Preferred Void Distributions on Void Measurements," ANL-5462 (April, 1955), p. 6.

8. Michael Petrick, "Two-Phase Air-Water Flow Phenomena," ANL-5787 (March, 1958).

9. B. L. Richardson, "Some Problems in Horizontal Two-Phase, Two-Component Flow," PhD Thesis, Purdue University.